Small-Angle Neutron Scattering Studies of Charged Carboxyl-Terminated Dendrimers in Solutions

Q. R. Huang,*,† P. L. Dubin,*,§ J. Lal,‡ C. N. Moorefield,|| and G. R. Newkome||

Department of Food Science, Rutgers University, 65 Dudley Road, New Brunswick, New Jersey 08901, Intense Pulsed Neutron Source Division, Argonne National Laboratory, Argonne, Illinois 60439, Department of Chemistry, Indiana University-Purdue University at Indianapolis, Indianapolis, Indiana 46202, and Departments of Chemistry and Polymer Science, University of Akron, Akron, Ohio 44325-4717

Received July 16, 2004. In Final Form: January 15, 2005

Small-angle neutron scattering was used to characterize the solution behavior of charged carboxylic acid terminated "cascade" dendrimers (Z-Cascade/methane [4]/3-oxo-6-oxa-2-azaheptylidyne/3-oxo-2-azaheptylidyne/propanoic acids) of third (G3) and fifth (G5) generations as a function of dendrimer concentration, pH, and ionic strength. An increase in dendrimer concentration leads to a single broad peak in the scattering profile arising from interdendrimer interaction. The dissociation of terminal carboxylate groups also gives rise to an interdendrimer interaction peak, which could be suppressed by the addition of excess salt. The results of contrast matching measurements indicate the accumulation of an excess concentration of tetramethylammonium counterions around the surface of these highly charged particles, and the thickness of these counterions lies somewhere between 4 and 6 Å. This conclusion is consistent with our previous potentiometric titration (Zhang, H.; et al. *J. Phys. Chem. B* **1997**, *101*, 3494) and capillary electrophoresis (Huang, Q. R.; et al. *J. Phys. Chem. B* **2000**, *104*, 898) data.

Introduction

Dendrimers, synthesized by controlled, repetitive reaction sequences, are densely branched molecules of well-defined spherical or nearly-spherical geometry.[1,2] Early studies of dendrimers were primarily focused on the design and synthesis of different kinds of dendrimers[3−9] and possible applications in various roles including recyclable chemical catalysts[10] and genetic transfer agents.[11,12] Because many of the applications and physical properties of dendrimers depend directly on the structural features of the dendrimers, such as the location and accessibility of the terminal functional groups, several experimental methods, such as size-exclusion chromatography (SEC),[13] viscometry,[13] transmission electron microscopy (TEM),[14] dynamic light scattering (DLS),[15] atomic force microscopy,[16] small-angle X-ray scattering,[17] and small-angle neutron scattering (SANS),[18−25] have been used in recent years to characterize dendrimers.

Carboxyl-terminated "cascade" dendrimers (Z-Cascade: methane [4]/3-oxo-6-oxa-2-azaheptylidyne/3-oxo-2-azaheptylidyne/propanoic acids) provide optimal models for small highly charged colloids. Within the realm of achievable synthesis (precluding branch defects), the range of molecular weights is 10^3-10^5, corresponding to radii of 1−5 nm.[4] They have well-defined functional end groups but no interior titratable groups.[26] Thus, for example, dendrimer−polyelectrolyte systems can provide a paradigm for the polyelectrolyte−colloid interactions that play an important role in the binding of proteins to DNA or

* To whom correspondence should be addressed.
† Rutgers University.
‡ Argonne National Laboratory.
§ Indiana University-Purdue University at Indianapolis.
|| University of Akron.

(1) Newkome, G. R.; Moorefield, C. N. In *Advances in Dendritic Macromolecules*; Newkome, G. R., Ed.; JAI Press: Greenwich, CT, 1993; Chapter 1.
(2) Newkome, G. R.; Moorefield, C. N.; Vögtle, F., *Dendrimers and Dendrons: Concepts, Syntheses, Applications*; Wiley-VCH: Weinheim, Germany, 2001.
(3) (a) Newkome, G. R.; Young, J. K.; Baker, G. R.; Potter, R. L.; Audoly, L.; Cooper, D.; Weis, C. D.; Morris, K.; Johnson, C. S., Jr. *Macromolecules* **1993**, *26*, 2394. (b) Kuzdzal, S. A.; Monnig, C. A.; Newkome, G. R.; Moorefield, C. N. *J. Chem. Soc., Chem. Commun.* **1994**, 2139.
(4) Young, J. K.; Baker, G. R.; Newkome, G. R.; Morris, K. F.; Johnson, C. S., Jr. *Macromolecules* **1994**, *27*, 3464.
(5) Newkome, G. R.; Moorefield, C. N.; Keith, J. M.; Baker, G. R.; Escamilla, G. H. *Angew. Chem. Int. Ed. Engl.* **1994**, *33*, 666.
(6) Tomalia, D. A.; Naylor, A. M.; Goddard, W. A., III. *Angew. Chem. Int. Ed. Engl.* **1990**, *29*, 138.
(7) Fréchet, J. M. J.; Gitsov, I. *Macromol. Symp.* **1995**, *98*, 441.
(8) Fréchet, J. M. J.; Hawker, C. J.; Wooley, K. L. *J. Mater. Sci.−Pure Appl. Chem.* **1994**, *31*, 1627.
(9) Hawker, C. J.; Lee, R.; Fréchet, J. M. J. *J. Am. Chem. Soc.* **1991**, *113*, 4583.
(10) Kukowskalatallo, J. F.; Bielinska, A. U.; Johnson, J.; Spindler, R.; Tomalia, D. A.; Baker, J. R. *Proc. Natl. Acad. Sci. U.S.A.* **1996**, *93*, 4897.
(11) Plank, C.; Mechtler, K.; Szoka, F. C.; Wagner, E. *Hum. Gene Ther.* **1996**, *7*, 1437.
(12) Service, R. F. *Science* **1995**, *267*, 458.
(13) Shah, G.; Dubin, P. L.; Kaplan, J. I.; Newkome, G. R.; Moorefield, C. N.; Baker, G. R. *J. Colloid Interface Sci.* **1996**, *183*, 397.
(14) Jackson, C. J.; Chanzy, H. D.; Booy, F. P.; Drake, B. J.; Tomalia, D. A.; Bauer, B. J.; Amis, E. J. *Macromolecules* **1998**, *31*, 6259.
(15) Valachovic, D. E.; Tomalia, D. A.; Amis, E. J. *Polym. Prepr.* **1995**, *36* (1), 373.
(16) Li, J.; Piehler, L. T.; Qin, D.; Baker, Jr., J. R.; Tomalia, D. A.; Meier, D. J.; *Langmuir* **2000**, *16*, 5613.
(17) Prosa, T. J.; Bauer, B. J.; Amis, E. J.; Tomalia, D. A.; Scherrenberg, R. *J. Polym. Sci., Part B: Polym. Phys.* **1997**, *35*, 2913.
(18) Nisato, G.; Ivkov, R.; Amis, E. J. *Macromolecules* **1999**, *32*, 5895.
(19) Amis, E. J.; Topp, A.; Bauer, B. J.; Tomalia, D. A. *ACS PMSE Prepr.* **1997**, *77*, 183.
(20) Scherrenberg, R.; Coussens, B.; van Vliet, P.; Edouard, G.; Brackman, J.; de Brabander, E. *Macromolecules* **1998**, *31*, 456.
(21) Ramzi, A.; Scherrenberg, R.; Brackman, J.; Joosten, J.; Mortensen, K. *Macromolecules* **1998**, *31*, 1621.
(22) Likos, C. N.; Rosenfeldt, S.; Dingenouts, N.; Ballauff, M.; Lindner, P.; Werner, N.; Vögtle, F. *J. Chem. Phys.* **2002**, *117*, 1869.
(23) Rosenfeldt, S.; Dingenouts, N.; Ballauff, M.; Lindner, P.; Likos, C. N.; Werner, N.; Vögtle, F. *Chem. Phys.* **2002**, *203*, 1995.
(24) Li. Y.; McMillan, C. A.; Bloor, D. M.; Penfold, J.; Warr, J.; Holzwarth, J. F.; Wyn-Jones, E. *Langmuir* **2000**, *16*, 7999.
(25) Bodnar, I.; Silva, A. S.; Deitcher, R. W.; Weisman, N. E.; Kim, Y. H.; Wagner, N. J. *J. Polym. Sci., Part B: Polym. Phys.* **2000**, *38*, 857.
(26) Zhang, H.; Dubin, P. L.; Kaplan, J.; Moorefield, C. N.; Newkome, G. R. *J. Phys. Chem. B* **1997**, *101*, 3494.

10.1021/la048207j CCC: $30.25
Published on Web 03/05/2005

ionic polysaccharides and in water treatment, papermaking, or dispersion stabilization of paints and cosmetics.

The "ideal" electrostatic behavior of these "cascade" dendrimers has been demonstrated by the analysis of their titration curves.[13,26] Thus, carboxyl-terminated dendrimers behave as spheres with uniform surface charge densities that can be modulated continuously by pH. Recently, we have characterized carboxyl-terminated dendrimers by potentiometric titration,[13] DLS,[26] and capillary electrophoresis[27] and found perfect adherence to the Poisson−Boltzmann equation under conditions of low charge.[26] However, for dendrimers of higher generation (≥2), a strong accumulation of counterions (counterion binding) is induced on the surface. The consequence of counterion binding is that the effective surface charge density is much weaker than the apparent geometric (or "structural") surface charge density.[26,27] However, none of the techniques mentioned above give direct information about the spatial distribution of the counterions.

Because electrostatic interactions strongly depend on the distribution of counterions around colloidal particles, this phenomenon is one of the most important factors affecting the behavior of colloid solutions. Potentiometric titration[26] and capillary electrophoresis[27] can only indirectly provide information about counterion binding. SANS is an established technique for investigation of the structure and distribution of small particles and is particularly effective for the study of aqueous dispersions,[28,29] as shown in previous studies on polyamidoamine (PAMAM)[18,19] or poly(propylene imine) [DAB-dendr-$(NH_2)_x$] dendrimers.[20,21] However, both systems contain interior tertiary amines, which complicates the relationship between pH and the degree of dissociation of protonated surface amine groups (α). For this reason, we focus here on the SANS of carboxyl-terminated dendrimers. Because it is possible to isolate the scattering of the dendrimers from that of their counterions by means of contrast variation methods, SANS in principle could provide important information about the counterion distribution around these highly charged particles. In this paper, we investigate the influence of dendrimer concentration, pH, and salt concentration on intermolecular interaction in solutions of G3 and G5. We use the bulky tetramethyl-d_{12}-ammonium ion instead of Na^+ or K^+ as the counterion to avoid specific ion-binding effects. The effect of pH on the spatial distribution of counterions (tetramethyl-d_{12}-ammonium) around G5 is presented.

Experimental Section

Materials. Carboxylic acid terminated cascade polymers (Z-Cascade/methane [4]/3-oxo-6-oxa-2-azaheptylidyne/3-oxo-2-azaheptylidyne/propanoic acids) of generations 3 and 5 (hereafter referred to as dendrimers) were synthesized by procedures described elsewhere.[3] G5 was further purified by dialysis (Spectra/Por dialysis membrane with a molecular weight cutoff equal to 1000), followed by freeze-drying.

Tetramethyl-d_{12}-ammonium chloride (>98 atom % D) (TMADCl) was purchased from Isotec, Inc. (Miamisburg, OH). Deuterium oxide (99.9 atom % D), tetramethylammonium hydroxide pentahydrate ($C_4H_{13}NO{\cdot}5H_2O$, purity > 97%), and tetramethylammonium chloride (purity ≥ 97%) were all from Aldrich Chemicals (Milwaukee, MI). Milli-Q water was used throughout this work. Table 1 shows the characteristics of the materials used.

Table 1. Properties of Materials Used

species	no. of terminal −COOH	MW (g/mol)	$\sum b$ (10^{-12} cm)	ρ (10^{-10} cm^{-2})
D_2O		20	1.9153	6.3928
H_2O		18	−0.1677	−0.5611
G3	108	12,345	261.55	1.2759
G5	972	111,373	2369.7	1.2813
TMADCl		121.5	116.04	8.29

Potentiometric Titration. The pH of dendrimer solutions was measured with a Beckman Φ34 pH meter equipped with a combination electrode under a nitrogen atmosphere at 25 ± 1 °C. The degree of ionization α of the carboxylic groups of a dendrimer is defined as

$$\alpha = \frac{[-COO^-]}{[-COOH] + [-COO^-]} \tag{1}$$

DLS Measurements. DLS measurements were performed using a DynamicPro-801 (Protein Solutions, Inc., Charlottesville, VA), equipped with a 790-nm solid-state laser of 30-mW power and an avalanche photodiode detector. All solutions were filtered with 0.1-μm Anotop filters (Whatman) into the 7-μL cell. The intensity−intensity autocorrelation function $G(\tau)$ is related to the electric field correlation function $g(q,t)$ by the Siegert relation:[30]

$$G(q,t) = A[1 + bg^2(q,t)] \tag{2}$$

where A is the experimental baseline and b is the spatial coherence factor which depends on the scattering geometry and details of the detection system. The constrained regulation method (CONTIN) developed by Provencher[31] was used to obtain the relaxation rate distribution function $A(\Gamma)$. The diffusion coefficient D was calculated according to $D = \Gamma q^2$, where q is the amplitude of the scattering vector defined as $q = (4\pi n/\lambda)\sin(\theta/2)$, n is the solution refractive index, λ is the laser wavelength, and θ is the scattering angle. The diffusion coefficient D can be converted into the hydrodynamic radius R_h using the Stokes−Einstein equation:

$$R_h = \frac{kT}{6\pi\eta D} \tag{3}$$

where k is the Boltzmannn constant, T is the absolute temperature, and η is the solvent viscosity.

SANS Measurements. SANS experiments were performed at the Intense Pulsed Neutron Source at Argonne National Laboratory, Argonne, IL, using the small-angle diffractometer (SAD).[32] The SAD instrument uses a multiple-aperture collimator consisting of a crossed pair of converging Soller collimators, one for vertical definition and the other for horizontal definition of the angular distribution, with the wavelength resolution $\Delta\lambda/\lambda$ ranging from 5 to 25%. SANS measurements were made for two dendrimers G3 and G5, with the G3 concentration fixed at 2.5% (v/v) and the G5 concentration ranging from 0.27 to 2.2% (v/v), at 25.0 ± 0.1 °C. The solutions were contained in a quartz sample holder with a thickness of 2 mm for most of the measurements except for the contrast matching experiments, where 1-mm-thick sample cells were used. In contrast matching experiments, 1% (v/v) G5 solution was first dissolved in a D_2O-H_2O mixture [26.5/73.5% (v/v)] and then TMADCl was added until the salt concentration reached 0.2 M. The 1 M TMAOH was used to adjust the pH. Under this contrast condition, G5 was matched out with the solvent; the information about the distribution of counterions TMAD was thus obtained. The data were recorded in the q range of 0.005−0.5 Å and corrected for detector efficiency, background scattering, and empty cell. The raw data were deduced following

(27) Huang, Q. R.; Dubin, P. L.; Moorefield, C. N.; Newkome, G. R. *J. Phys. Chem. B* **2000**, *104*, 898.
(28) Hodge, D. J.; Laughlin, R. G.; Ottewill, R. H.; Rennie, A. R. *Langmuir* **1991**, *7*, 878.
(29) *Neutron, X-Ray and Light Scattering: Introduction to an Investigative Tool for Colloidal and Polymeric Systems*; Lindner, P., Zemb, Th., Eds.; North-Holland, Amsterdam, 1991.
(30) (a) Schmitz, K. *Dynamic Light Scattering by Macromolecules*; Academic Press: New York, 1990; Chapter 10. (b) Berne, B. J.; Pecora, R. *Dynamic Light Scattering with Application to Chemistry, Biology and Physics*; Wiley: New York, 1976.
(31) Provencher, S. W. *Comput. Phys. Commun.* **1982**, *27*, 229.
(32) Thiyagarajan, P.; Epperson, J. E.; Crawford, R. K.; Carpenter, J. M.; Klipper, T. E.; Wozniak, D. G. *J. Appl. Crystallogr.* **1997**, *30*, 280.

the procedures described in ref 32. The incoherent background level in the samples was estimated by subtracting the intensity level at a sufficiently large value of q (> 0.3 Å), which is a constant.

Results and Discussion

Effect of Concentration. The small-angle scattering cross section per unit volume, $I(q)$, for a monodisperse colloid solution can be written as[33]

$$I(q) = n_p \Delta\rho^2 P(q)\, S(q) \tag{4}$$

where $q = (4\pi/\lambda)\sin(\theta/2)$ is the scattering vector, λ is the wavelength of the radiation, θ is the scattering angle, n_p is the number density of the dendrimers in solution, and $\Delta\rho^2$ is the contrast factor given by

$$\Delta\rho^2 = \left(\frac{\sum_d b_i}{v_d} - \frac{\sum_s b_i}{v_s}\right)^2 \tag{5}$$

where $\sum_d$ and $\sum_s$ are summation of the scattering lengths b_i of the different atoms in the molecules and v_d and v_s are the molecular volumes of the dendrimer and the solvent molecules, respectively. One defines the scattering length density ρ as $\rho = \sum_i b_i/v$. The ρ values for different materials are listed in Table 1. The quantity $P(q) = |F(q)|^2$ is the form factor (or the intraparticle structure factor), and $S(q)$ is the interparticle structure factor.[34] In a suspension of weak interaction or in a dilute solution $S(q) \sim 1$, and in the low-q regime ($qR_g < 1$), the scattering intensity given by eq 4 can generally be analyzed by the classical Guinier method to obtain the radius of gyration (R_g). The Guinier approximation at low q can be described as[35]

$$I(q) = I(0)\exp\left(-\frac{q^2 R_g^2}{3}\right) \tag{6}$$

For a monodisperse spherical particle with a radius R, the form factor can be described as[36]

$$P(q) = \left[3\frac{\sin(qR) - qr\cos(qR)}{(qR)^3}\right]^2 \tag{7}$$

Figure 1 shows the semilogarithmic plot of the scattering intensity normalized with respect to concentration as a function of concentration for G5 in D_2O at pH = 9.00 (α = 1.0). At high q values, the scattered intensities collapse to a single curve which shows $q^{-3.5} \pm 0.2$ variation. This power relationship indicates that the dendrimer surface is somewhat fuzzy, in contrast to the perfectly sharp interface (q^{-4} variation, Porod's law). This q regime contains information about the local structure within the dendrimer molecule and indicates that the internal structure of the dendrimer is not influenced significantly by intermolecular interactions.[21] At low concentration [i.e., C = 0.27% (v/v)], the scattering curve corresponds to independent noninteracting particles. The intensity $I(q \rightarrow 0)$ can be described as $I(q \rightarrow 0) \sim k_B T(\partial\phi/\partial\Pi)_T$

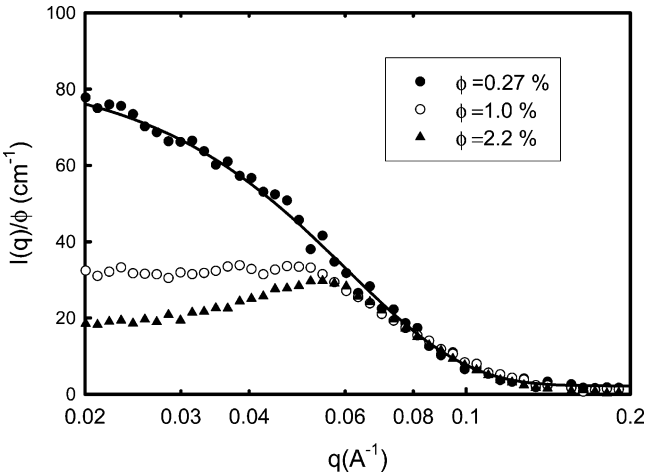

Figure 1. Scattering intensity from carboxyl-terminated dendrimers G5 in D_2O at different G5 concentrations: 0.27% (v/v; solid circles); 1.0% (v/v; empty circles); and 2.2% (v/v; solid triangles). Uncertainties of the data are within the size of the symbols.

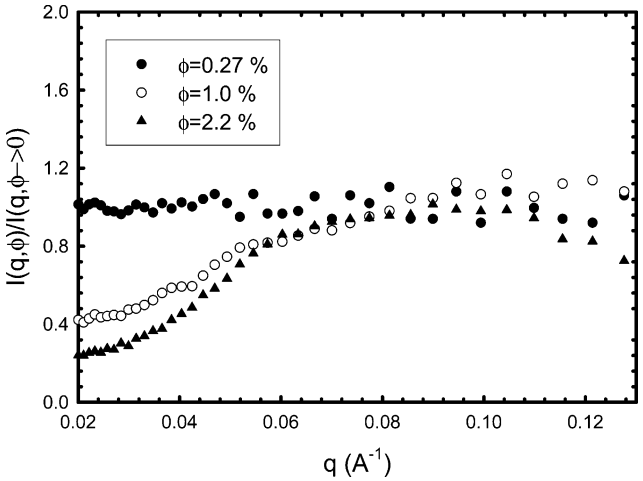

Figure 2. Plot of the scattering intensities divided by the form factor of the dendrimer G5 extrapolated to zero concentration (cf. Figure 1).

$\sim \phi(1+A_2\phi)$,[37] where k_B is the Boltzmann constant, Π is the osmotic pressure of the solution, and A_2 is the second virial coefficient. However, at higher concentration [C > 1% (v/v)], a weak peak appears and becomes more pronounced with an increase of concentration. The appearance of the peak in the $I(q)$ versus q curve originates from interparticle long-range electrostatic interactions typical of highly charged colloids.[38] The position of the peak depends on the spatial arrangement of the particles and on the geometrical structure of each particle (i.e., interparticle and intraparticle interferences).[36] One can estimate the effect of the concentration on interparticle interactions, that is, the structure factor $S(q)$, by dividing $I(q)$ by the dendrimer form factor described in eq 4, where the scattered intensity corresponding to ϕ = 0.27% (v/v) is approximated by the $\phi \rightarrow 0$ form factor, as shown in Figure 2. One notes a strong correlation in the interdendrimer structure factor at low q, which arises from the decrease in the isothermal compressibility with increased concentration.[21] The weak peak is due to the structure of charged

(33) (a) Bendedouchi, D.; Chen, S. H. *J. Phys. Chem.* **1983**, *87*, 1653; (b) Kotlarchyk, M.; Chen, S.-H. *J. Chem. Phys.* **1983**, *79*, 2481.
(34) Chen, S.-H.; Lin, T. L. In *Methods of Experimental Physics-Neutron Scattering in Condensed Matter Research*; Skold, K., Price, D. L., Eds.; Academic Press: New York, 1987; Vol. 23B, Chapter 16.
(35) Guinier, A.; Fournet, G. *Small Angle Scattering of X-rays*; John Wiley and Sons: London, 1955.
(36) Chen, S.-H. *Annu. Rev. Phys. Chem.* **1986**, *37*, 351.
(37) Higgins, J. S.; Benoit, H. C. *Polymers and Neutron Scattering*; Clarendon Press: Oxford, 1994.
(38) Schmitz, K. S. *Macroions in Solution and Colloidal Suspension*; VCH Publishers: New York, 1993.

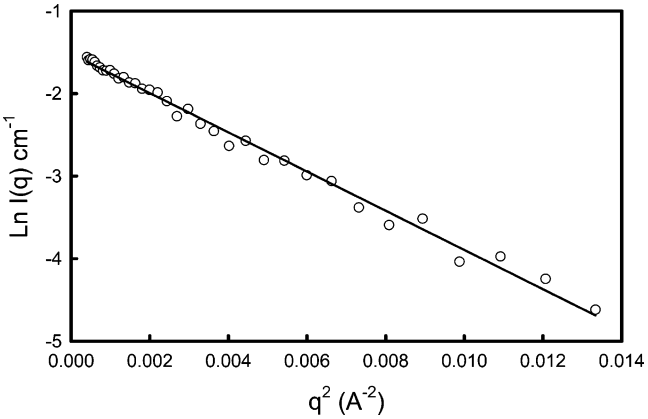

Figure 3. Guinier representation of the scattering intensity from 0.27% (v/v) G5 solution in D_2O at pH = 9.00.

dendrimers in solution with an intensity decrease at low q showing repulsive interaction between dendrimers. We can estimate the average interparticle distance (d) using[36]

$$d = 1.22(2\pi/q_{max}) \quad (8)$$

For 2.2% (v/v), d is about 14 nm.

Numerous studies, including matrix-assisted laser desorption ionization time-of-flight mass spectrometry, SEC, TEM, and diffusion-ordered spectroscopy NMR on the carboxyl-terminated, as well as mass spectrometry and NMR on their ester precursors, indicate that these molecules are spherical and that the samples are monodisperse.[2,3] To obtain the dendrimer size, we analyze the SANS data using the Guinier plot for 0.27% (v/v) G5 in D_2O at pH = 9.00, as shown in Figure 3. The ln $I(q)$ is linear with q^2 over a wide range of scattering vectors q, the slope of this line leading to R_g of 2.7 ± 0.1 nm. Fitting the scattering data with the monodisperse spherical model in the regime $qR > 1$ using eq 7 gives R = 3.1 ± 0.2 nm. Similarly, we obtain the R value for 2.5% (v/v) G3 at pH = 4.04 of 1.5 ± 0.1 nm. Using a Gaussian size distribution of spheres,[39] the results show low polydispersity ($p < 10\%$) for both G3 and G5, in agreement with the findings[2,3] noted above.

Hydrodynamic radii for G5 and G3 were found by NMR to be 3.2 and 1.7 nm, respectively.[3,4] The R_g/R_h ratios for our G5 and G3 are equal to 0.87 and 0.88, respectively, while that of a uniform-density solid sphere is 0.775.[40] Previous studies on generation 5 of DAB-dendr-$(NH_2)_{64}$[21] and generations 4, 7, and 8 of PAMAM[35] yield R_g/R_h ratios of 0.702, 0.74, 0.88, and 1.00, respectively. Values higher than the ideal sphere value could be due to the higher segment density near the exterior of the dendrimers.[21,41]

Effect of pH. Figure 4 shows the typical scattering curves of G3 at pH = 4.04 and 8.32 in I = 0.2 M TMADCl/D_2O. A solvent ionic strength of 0.2 M was used so that the pH could be adjusted with 1 M TMAOH without dramatic changes in ionic strength. At low pH, the scattering curve resembles that of a noninteracting particle; at high pH, a broad peak appears in the scattering. In this strongly interacting system, the Guinier method is no longer adequate to determine the size of the particles. Thus, to obtain the effective size as a function of pH we use monodisperse sphere fits of scattering in the limit of

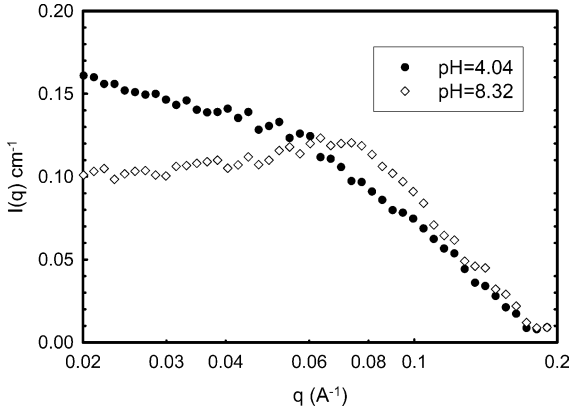

Figure 4. Effect of pH on the scattering intensity from a 2.5% (v/v) G3 solution in 0.2 M TMADCl/D_2O: pH = 4.04 (solid circles) and pH = 8.32 (empty circles).

Table 2. Effect of pH on the Effective Radius of 2.5% (v/v) G3

PH	radius (nm)	PH	radius (nm)	PH	radius (nm)
4.04	1.5 ± 0.2	6.32	1.3 ± 0.2	8.32	1.4 ± 0.2
4.87	1.3 ± 0.2				

$qR > 1$, where the interparticle interactions are negligible. Table 2 shows that effective sizes of 2.5% (v/v) G3 are independent of pH. This result is in agreement with findings of Amis et al.[42] who reported no dependence on either pH or ionic strength for the G8 (PAMAM) dendrimer and at variance with the results of simulations as noted in ref 42.

Amis et al. reported that the two distinct diffusive modes in the intensity−intensity autocorrelation function for spherical dendrimers in the low-salt limit were, in a manner similar to the observation for linear polyelectrolytes, due to the effects of electrostatic interactions.[43,44] While we also observe two modes in DLS, we found the second mode (slow mode) to be filterable. Figure 5 shows the CONTIN results of 2.5% (v/v) G3 in D_2O with filter sizes of 0.1 and 0.02 μm. For the first case, there are clearly two modes; however, the slow mode disappears if the 0.02-μm filter is used. The origin of the mysterious slow mode is beyond the scope of our current paper.

Distribution of Counterions. That the interdendrimer interaction peak can be suppressed by the addition of excess salt is consistent with the screening of the electrostatic interaction by salt, a common feature of colloid solutions. This result in itself does not distinguish the usual Debye−Hückel screening from the more localized counterion "binding", or Manning-type "condensation", previously invoked to explain the anomalously low electrophoretic mobility of high-generation carboxyl-terminated dendrimers.[26,27] Contrast-matching SANS makes it possible to distinguish the counterion signal from that of the dendrimer, providing a way to identify the presence of a counterion-rich layer surrounding the colloidal particle. We used the deuterated salt TMADCl and matched the contrast factor of dendrimer with the solvent [26.5:73.5% D_2O/H_2O (v/v)] to render it invisible. In the contrast-matched case, the scattering is purely from the counterion atmosphere, whereas in pure D_2O, the scattering arises predominantly from the contribution of the dendrimer core (cf. Table 1). The relatively weak scattering under the contrast-matching condition of 73.5% (v/v)

(39) Bendedouch, D.; Chen, S.-H.; Koehler, W. C. *J. Phys. Chem.* **1983**, *87*, 153.
(40) Yamakawa, H. *Modern Theory of Polymer Solutions;* Harper & Row: New York, 1971
(41) Bauer, B. J.; Briber, R. M.; Hammouda, B.; Tomalia, D. A. *Polym. Mater. Sci. Eng*. **1992**, *67*, 428.
(42) Nisato, G.; Ivkov, R.; Amis, E. J. I. *Macromolecules* **2000**, *33*, 4172.
(43) Sedlak, M.; Amis, E. J. *J. Chem. Phys*. **1992**, *96*, 817.
(44) Sedlak, M.; Amis, E. J. *J. Chem. Phys.* **1992**, *96*, 826.

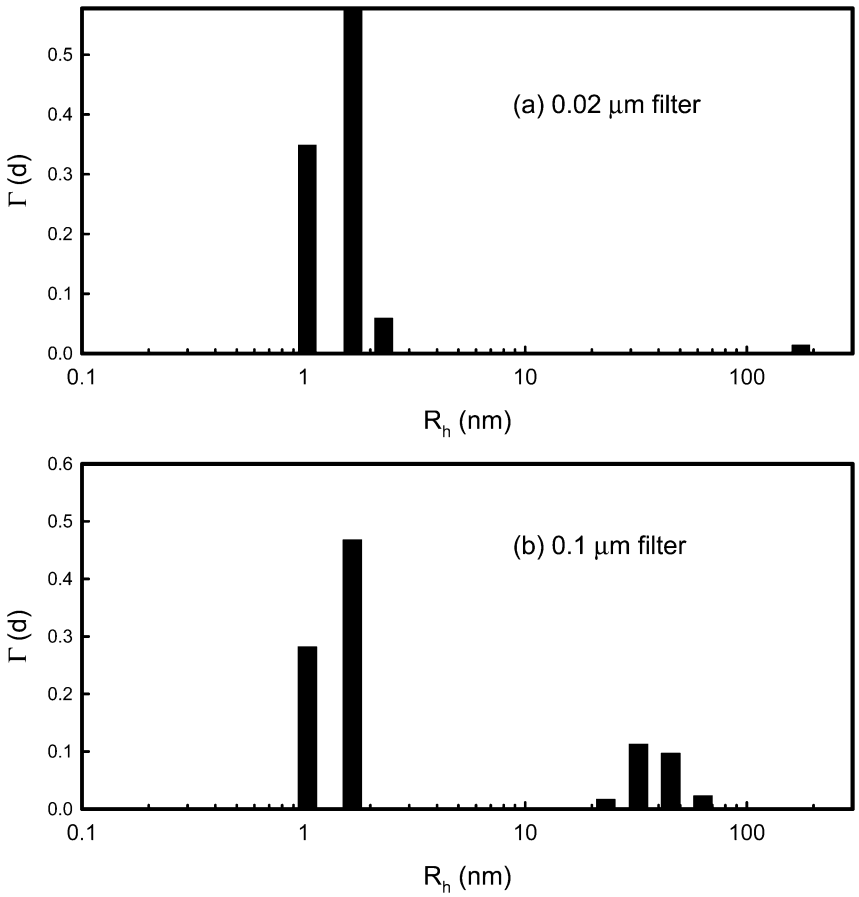

Figure 5. DLS results of the size distribution (CONTIN) of 2.5% (v/v) G3 solutions in D_2O prepared with different filter sizes: (a) 0.02-μm filter and (b) 0.1-μm filter.

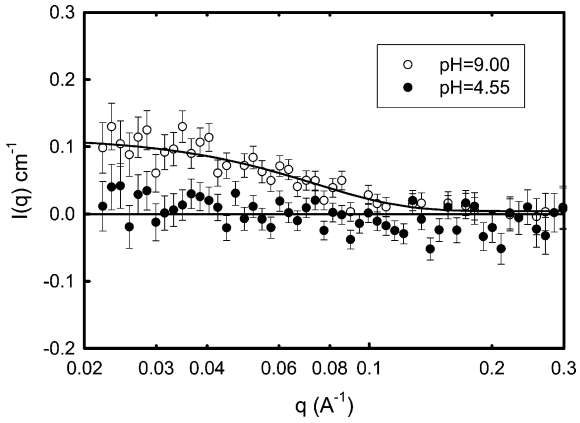

Figure 6. Effect of pH on the scattering intensity from counterions 0.2 M $TMAD^+$ of 1.0% (v/v) G5 in a 26.5:73.5% D_2O/H_2O (v/v) mixed solvent, where G5 is contrast-matched by the mixture: pH = 4.55 (solid circles) and pH = 9.00 (empty circles). The solid line is the fit to eq 6.

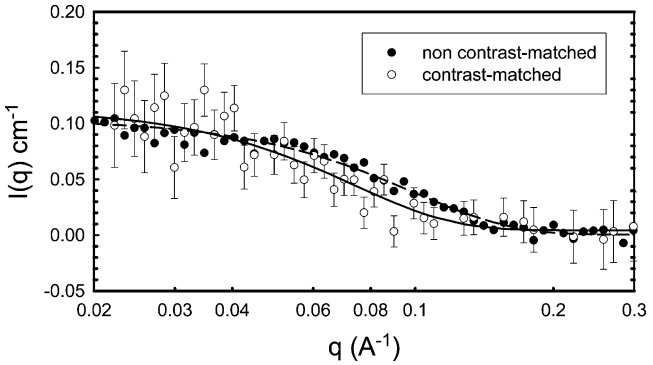

Figure 7. Scattering from 1.0% (v/v) G5 at pH = 9.00 with 0.2 M TMADCl salt under the contrast-matched condition [26.5: 73.5% D_2O/H_2O (v/v), empty circles] and non-contrast-matched condition (pure D_2O, solid circles). Solid lines are fits to eq 6.

hydrogenated water and the relatively low neutron flux lead to a low signal-to-noise ratio and, therefore, mandate a careful statistical analysis of the data. Nevertheless, the resulting SANS scattering profile, which reflects the spatial distribution of $TMAD^+$ interacting with dendrimers, provides some unique semiquantitative insight into the distribution of counterions around a highly charged sphere, something not directly observable by other methods.

Figure 6 shows the effect of pH on the scattering curves due to the counterions. At low pH (i.e., 4.55), there is no q dependence of the scattered intensity $I(q)$, which indicates that G5 is successfully matched out by D_2O, and the small counterions $TMAD^+$ are homogeneously distributed in the solution. However, at high pH (i.e., 9.0) when the COOH groups are totally dissociated, the scattering profile is radically different from that at low pH: a dramatic increase in coherent scattering occurs which can only be attributed to buildup of counterions near the surface of highly charged G5. This counterion localization is seen upon comparing the scattering profile for fully charged contrast-matched G5 to that in pure D_2O, as shown in Figure 7. The shift to lower q for the contrast-matched sample reflects the formation of a larger spherical particle as $TMAD^+$ ions accumulate in the vicinity of G5. Despite the large apparent scatter, t-test analysis[45] of the

(45) See http://psych.rice.edu/online_stat/chapter8/difference_means.html.

data shows that the differences in the slopes is statistically significant, so the Guinier method (eq 6) can be applied to the two conditions with proper attention to error limits. The result is a value of $R_g = 23$ (± 2) Å for the counterion shell, compared to the value of $R_g = 18$ (± 1) Å obtained in pure D_2O, where only the core of the dendrimer is observed (the numbers in parentheses are standard deviations). The difference between the fitted values of 23 and 18 Å for the two sets of data ΔR is 5 ± 1 Å, where the indicated range corresponds to the 95% confidence level in ΔR.[45] While an explicit structural interpretation would clearly be more robust with more precise scattering data, it is certainly noteworthy that an accumulation of TMA^+ counterions in a region whose outer boundary lies about 0.5 nm from the dendrimer surface would be consistent with previous capillary electrophoresis and potentiometric measurements.[26,27] In those studies, a simlar counterion domain was proposed to explain the reduction of both the zeta potential and the surface potential relative to the values expected for a bare sphere with the radius and structural charge of this dendrimer.

Conclusions

SANS has been used to study solutions of third (G3) and fifth (G5) generation carboxyl-terminated dendrimers, in D_2O with tetramethyl-d_{12}-ammonium chloride (TMADCl). SANS results indicate that both G3 and G5 are nearly monodisperse, spherical particles. When the dendrimer concentration is increased, a single broad peak due to interdendrimer interaction appears in the scattering profile. An increase in pH also gives rise to an interference peak, while the radius changes only slightly with pH. As expected, electrostatic interactions may be screened by the addition of excess salt. Contrast matching studies reveal the accumulation of counterions around the surface of highly charged G5. This result is consistent with the anomalously low mobilities and the suppression of surface potential for G5 found, respectively, in previous capillary electrophoresis and potentiometric titration studies.

Acknowledgment. We would like to thank Ed Lang at IPNS for his technical support during the SANS measurements. This work was supported by the National Science Foundation through Grants DMR 0076068 (P.L.D.) and DMR 0196231 (G.R.N.) as well as AFOSR (F49620-02-1-0428) (G.R.N.) and ACS-PRF (41333-G7) (Q.R.H.).

LA048207J